

# Nanorotors using asymmetric inorganic nanorods in an optical trap

Manas Khan<sup>1</sup>, A K Sood<sup>1</sup>, F L Deepak<sup>2</sup> and C N R Rao<sup>2</sup>

<sup>1</sup> Department of Physics, Indian Institute of Science, Bangalore-560012, India

<sup>2</sup> Chemistry and Physics of Materials Unit, Jawaharlal Nehru Centre for Advanced Scientific Research, Bangalore-560064, India

E-mail: [asood@physics.iisc.ernet.in](mailto:asood@physics.iisc.ernet.in)

Received 27 January 2006, in final form 10 March 2006

Published 19 May 2006

Online at [stacks.iop.org/Nano/17/S287](http://stacks.iop.org/Nano/17/S287)

## Abstract

We demonstrate how light force, irrespective of the polarization of the light, can be used to run a simple nanorotor. While the gradient force of a single beam optical trap is used to hold an asymmetric nanorod, we utilize the scattering force to generate a torque on the nanorod, making it rotate about the optic axis. The inherent textural irregularities or morphological asymmetries of the nanorods give rise to the torque under the radiation pressure. Even a small surface irregularity with non-zero chirality is sufficient to produce enough torque for moderate rotational speed. Different sized rotors can be used to set the speed of rotation over a wide range with fine tuning possible through the variation of the laser power. We present a simple dimensional analysis to qualitatively explain the observed trend of the rotational motion of the nanorods.

(Some figures in this article are in colour only in the electronic version)

## 1. Introduction

Optical manipulation of micron-sized particles has been a major success for more than a decade [1]. The technique of optical tweezers has now become an established tool in physics and single molecule biophysics. The ability to apply light force for generating torque on micro-objects making them rotate in a controlled fashion has great importance in optical micromachining and biotechnology. Various techniques have, therefore, been investigated to design optically driven microrotors. A few schemes in this field have already been reported [2–14]. In the new age of nanotechnology, it would obviously be a target to design a laser-assisted rotor using nanostructures. Here we report a simple scheme, complementary to the existing literature, describing how inorganic nanorods can be used to construct laser-assisted nanorotors.

First we briefly summarize the existing schemes and their range of applicabilities. In a circularly polarized optical trap, birefringent microparticles are seen to rotate [2, 3]. Microobjects, when trapped in a spiral optical pattern, have also been observed to rotate [4–6]. Rotations of specifically fabricated rather big rotors under an optical trap have been

reported [7–9]. Use of spatial light modulators (SLMs) is another novel way to rotate multi-particle structures [10] or to make optical vortex arrays which in turn cause rotation of spherical microparticles [11]. An asymmetric dumbbell-like structure of two colloidal particles also rotates in an optical trap [12]. Nanorods, trapped very close to the cover glass, can be rotated about their cross-sectional diameter by rotating the plane of polarization of light [13, 14].

We have trapped ZnO and Al<sub>2</sub>O<sub>3</sub> nanorods in a conventional single beam optical tweezers set-up using linearly polarized infrared light. The inherent surface irregularities or asymmetries in shape, bearing non-zero chirality, when exposed to the radiation pressure experience a net torque, making the trapped nanorod rotate about the optic axis. Rotations of different sized particles, ranged from a single nanorod to a bundle of nanorods, covering a wide spectrum of rotational speed, have been observed. We observed that even small extrusions on the surface of a nanorod are sufficient to generate enough torque to make the nanorod rotate at a moderate rotational speed. As those small irregularities are inbuilt to all synthesized nanorods and commonly do not have any mirror plane of symmetry passing through the optic axis, any of the nanorods can be used as a nanorotor under the laser

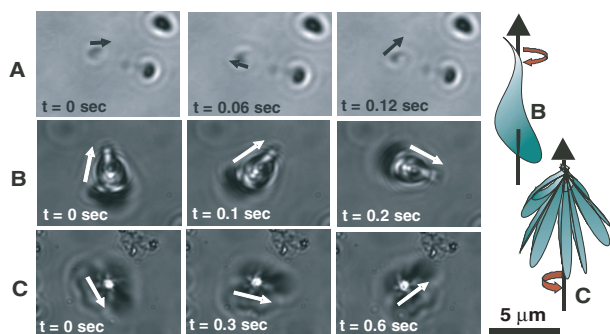


**Figure 1.** Time sequences of different sized and shaped rotors are shown here. In each time frame the orientation of the rotor is indicated by an arrow. Panels (A), (B) and (C) represent rotations of three  $\text{Al}_2\text{O}_3$  rotors. The rotor in panel (A) is a typical nanorod whereas the rotor in panel (B) is a bigger asymmetric nanorod, and in panel (C), the rotor is a nanorod bundle. The predicted structures of the rotors in panels (B) and (C) have been depicted in the rightmost column. A size bar has been shown at the bottom right-hand corner. Magnification factors of all the images are same. The images shown in panel (A) are diffraction-limited images and hence they do not convey the real size of the rotor.

trap. A rotor of suitable size and shape is chosen accordingly to set the rotational speed near a desired value and then by varying the trapping beam intensity the speed is finely adjusted. This scheme, therefore, provides a complete and precise control over the rotational speed of the nanorotors.

## 2. Experimental details

A 1064 nm linearly polarized laser beam from a 2.5 W Nd:YVO<sub>4</sub> laser was focused through a 1.4 numerical aperture 63 $\times$  objective to trap the nanorods with typical diameter 50–60 nm and length  $\sim 2 \mu\text{m}$ . The  $\text{Al}_2\text{O}_3$  nanorods were obtained by carbon-assisted synthesis [15, 16] starting with a mixture of Al powder and graphite/activated carbon (molar ratio 1:1). For the synthesis of ZnO nanorods, we have employed a procedure involving the solid-state reaction between zinc oxalate and multi-walled carbon nanotubes (MWNTs) [15, 16]. The nanorods were well dispersed in *N,N*-dimethylformamide by two hours of sonication. A drop of the nanorod suspension was taken on a transmission electron microscope (TEM) grid to observe the morphology of the nanorods. The inset of figure 2 shows a few TEM images of some typical  $\text{Al}_2\text{O}_3$  and ZnO nanoparticles. The images clearly show that the suspension contains nanorods of different asymmetric shapes or with surface irregularities and some odd bundles of nanorods. A few drops of the dispersion were taken in an annular chamber on a coverglass for observations. We have observed rotations of different types of rotors. The experiments were recorded at 30 frames  $\text{s}^{-1}$  with a digital CCD camera attached to the microscope. The rotational speeds of the nanoparticles were calculated from the recorded frames and thus the calculation was limited to a maximum value of speed  $\sim 10$  Hz. The rotational speeds of different sized and shaped single nanorods and nanorod bundles were studied at varying laser power. In many cases, the rotational speed or size of the rotors were beyond the maximum measurement capability through imaging technique. In figure 1 we show rotations of some typical rotors with different shapes and sizes.

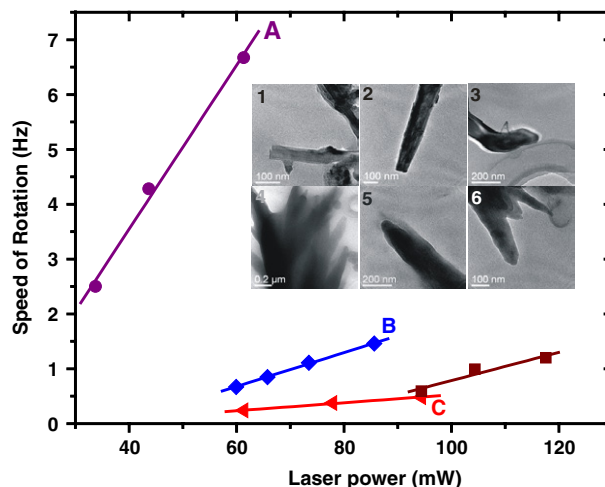


**Figure 2.** The graph shows the variation of rotational speed with laser power for four different  $\text{Al}_2\text{O}_3$  rotors. The plots labelled A, B and C correspond to the rotors shown in panels (A), (B) and (C) respectively in figure 1. The inset shows TEM images of some typical nanoparticles. Frames 1 and 2 show  $\text{Al}_2\text{O}_3$  nanorods with irregularities on the surface, and frame 3 displays an asymmetric  $\text{Al}_2\text{O}_3$  nanorod. A bundle of  $\text{Al}_2\text{O}_3$  nanorods is shown in frame 4. Frames 5 and 6 exhibit an asymmetric ZnO nanorod and a bundle of ZnO nanorods respectively.

## 3. Rotational speed–laser power relationship

The variation of the speed of rotation with laser power for some of the  $\text{Al}_2\text{O}_3$  rotors is shown in figure 2, corresponding to rotors in panels (A), (B) and (C) of figure 1. In all cases, the speed of rotation increases monotonically with the laser power and there is a non-zero finite value of the laser power at which the rotors start rotating. While the rotational speed of all the rotors follow a linear relationship with the laser power, the slope and the intercept depend on the size and shape of the rotor. The slope is steeper for small and more asymmetric rotors. Bigger rotors have a higher threshold value of laser power for the onset of rotation, along with a flatter variation of rotational speed with laser power. So it can be concluded that small rotors with large asymmetry have more efficiency at all laser power levels whereas the bigger rotors are not so effective at low laser power level as they need more laser power for starting up the rotation.

In addition to this, it is noteworthy that the direction of the rotational motion was not same for all the rotors. Though a rotor always rotated in a particular direction, both right-handed and left-handed rotations were observed with equal probability in randomly selected nanorotors.

## 4. Theoretical understanding

In figure 3 we depict a very simple model to qualitatively understand the rotational motion of the nanorods when trapped under linearly polarized laser beam. Most of the nanorods have surface irregularities or morphological asymmetries that do not have any symmetry about a mirror plane passing through the optic axis of the trapping beam. In a simple-minded way, here we model a nanorod as a cylinder with some extrusions on its surface. The nanorod is trapped at the point of focus by the gradient force of the tightly focused laser beam. For

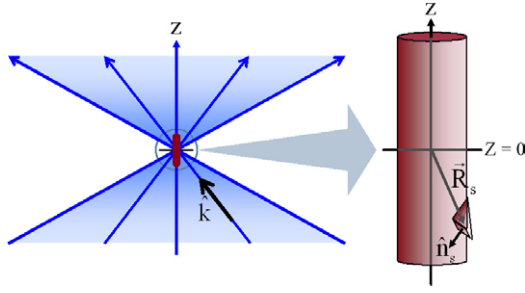


**Figure 3.** A model of a nanorod in the optical trap is shown here. An enlarged image of the nanorod is depicted at the right. It has a small extrusion with surface area  $s$  along  $\hat{n}_s = a\hat{r} + b\hat{\phi} + c\hat{z}$  at a position  $\vec{R}_s(r_s, \phi_s, z_s)$ .

simplicity, in figure 3 we have shown only one extrusion on the surface of the nanorod. As this extrusion is not symmetric about a plane passing through the  $z$ -axis, it will provide a non-zero chirality to the nanorod structure. Therefore, the radiation pressure force will generate a non-zero torque on the nanorod. The radial and the azimuthal component of the torque would be nullified by the gradient force and only the axial component would survive to provide a non-zero angular momentum to the nanorod causing its rotation about the optic axis. Now if the surface of the nanorod is full of randomly oriented extrusions, some would produce left-handed torque and the remaining ones would contribute to generate right-handed torque. So the net torque experienced by the nanorod is completely determined by the structure and morphology of the nanorod and hence the direction of rotation as well as the speed of rotation is different for different rotors. Since the absorbance of the inorganic nanorods at 1064 nm is negligible [17, 18], the deformation of the nanorods or any other effects caused by the sample heating are not considered here. The existence of a laser power threshold for the onset of rotation is a bit puzzling. We are unable to understand the origin of the threshold and why it increases with the increasing size of the rotors.

Calculating the electromagnetic field near the focus of a very large aperture beam, and around a particle itself which is neither very small nor very large compared to the wavelength of the radiation, is notoriously very difficult and hence the exact analysis of the radiation pressure force acting on the nanorods becomes nearly intractable. Hence we try to understand the trend of the observed rotational motion by a simple dimensional analysis.

The momentum density of radiation is given by  $\vec{g}(r, z) = \frac{1}{2c} \epsilon_0 E^2 \hat{k}$ , where  $E(r, z)$  is the magnitude of the electric field of light propagating along  $\hat{k}$ . So the radiation pressure force scales as  $E^2/c \equiv P/c$ , where  $P$  is the laser power and  $c$  is the velocity of light. For the nanorod shown in figure 3, the net torque generated in the laser trap can be given by

$$\vec{\tau} = 2Rc \int_s \vec{R}_s \times (-\hat{n}_s)(\vec{g} \cdot \hat{n}_s) ds \quad (1)$$

where  $R$  is the reflectance of the nanorod and the integration is done over the total area of the surface irregularities or extrusions. The larger extrusions with greater chirality would contribute more to the net torque. Hence, the magnitude of the

driving torque  $\tau$  will scale as

$$\tau \sim \chi \left( \frac{P}{c} \right) l. \quad (2)$$

Here  $\chi$  is a phenomenological parameter measuring the chirality and  $l$  is a size scale factor. Since here the Reynolds number is small ( $\sim 10^{-5}$ ), the Stokes equation can be used to get  $\vec{\tau} = D\vec{\Omega}$ , where  $D$  is the hydrodynamic drag coefficient and  $\Omega$  is the rotational speed. The drag coefficient for a cylindrical object rotating about its axis with cross-sectional radius  $r$  and length  $L$  is  $D = 4\pi\eta r^2 L$ , where  $\eta$  is the viscosity of the medium [19]. Therefore,  $D \sim l^3$  and the rotational speed  $\Omega$  of the rotor will scale as

$$\Omega \sim \chi \left( \frac{P}{c} \right) l^{-2}. \quad (3)$$

This equation qualitatively explains the observed trend of the rotational motion. For smaller rotors, the rotational speed increases more sharply with increasing laser power compared to the bigger rotors that show a flat variation of rotational speed with laser power. Thus at the same laser power a smaller rotor with more asymmetry (larger  $\chi$ ) would rotate faster.

## 5. Conclusion

Our observations and the qualitative explanation with dimensional analysis show that inorganic nanorods can be conveniently used as optically driven nanorotors. Different sized rotors can be chosen to cover different rotational speed regimes with the fine tuning made possible by varying the laser power. The inorganic nanorods provide a better choice as nanorotors since even small ones are easily trapped due to their high dielectric constants. The controllability, simplicity and flexibility of the rotational motion of these rotors suggest that this scheme can be applied universally to devise easy-to-use optically driven nanorotors. The availability of inorganic nanorods bearing the desired size and asymmetry would favour the present scheme to design nanorotors with predictable rotational speeds. Recent experiments on trapping and manipulation of carbon nanotubes [20–22] suggest that Y-junction nanotubes [23] may provide another interesting choice to be used as nanorotors under an optical trap. The nanorotors could be used in micropumps to guide fluids through microchannels or as microstirrers. This rotational motion can also be used in experiments related to microrheology and microfluidics.

## Acknowledgments

We thank the Department of Science and Technology, India, for support under the DST Nanoscience Initiative.

## References

- [1] Ashkin A, Dziedzic J M, Bjorkholm J E and Chu S 1986 *Opt. Lett.* **11** 288
- [2] Friese M E J, Nieminen T A, Heckenberg N R and Rubinsztein-Dunlop H 1998 *Nature* **394** 348
- [3] Cheng Z, Chaikin P M and Mason T G 2002 *Phys. Rev. Lett.* **89** 108303

- 
- [4] He H, Friese M E J, Heckenberg N R and Rubinsztein-Dunlop H 1995 *Phys. Rev. Lett.* **75** 826
- [5] Friese M E J, Enger J, Rubinsztein-Dunlop H and Heckenberg N R 1998 *Nature* **394** 348
- [6] Paterson L, MacDonald M P, Arlt J, Sibbett W, Bryant P E and Dholakia K 2001 *Science* **292** 912
- [7] Higurashi E, Ukita H, Tanaka H and Ohguchi O 1994 *Appl. Phys. Lett.* **64** 2209
- [8] Galajda P and Ormos P 2001 *Appl. Phys. Lett.* **78** 249
- [9] Galajda P and Ormos P 2002 *Appl. Phys. Lett.* **80** 4653
- [10] Eriksen R L, Rodrigo P J, Daria V R and Glückstad J 2003 *Appl. Opt.* **42** 5107
- [11] Ladavac K and Grier D G 2004 *Opt. Express* **12** 1144
- [12] Luo Z-P, Sun Y-L and An K-N 2000 *Appl. Phys. Lett.* **76** 1779
- [13] Bonin K D, Kourmanov B and Walker T G 2002 *Opt. Express* **10** 984
- [14] Bishop A I, Nieminen T A, Heckenberg N R and Rubinsztein-Dunlop H 2003 *Phys. Rev. A* **68** 033802
- [15] Rao C N R, Deepak F L, Gundiah G and Govindaraj A 2003 *Prog. Solid State Chem.* **31** 5
- [16] Gundiah G, Deepak F L, Govindaraj A and Rao C N R 2003 *Top. Catal.* **24** 137
- [17] Gu Y, Kuskovsky I L, Yin M, O'Brien S and Neumark G F 2004 *Appl. Phys. Lett.* **85** 3833
- [18] Innocenzi M E, Swimm R T, Bass M, French R H, Villaverde A B and Kokta M R 1990 *J. Appl. Phys.* **67** 7543
- [19] Cocco S, Monasson R and Marko J F 2002 *Phys. Rev. E* **66** 051914
- [20] Plewa J, Tanner E, Mueth D M and Grier D G 2004 *Opt. Express* **12** 1978
- [21] Tan S, Lopez H A, Cai C W and Zhang Y 2004 *Nano Lett.* **4** 1415
- [22] Khan M, Sood A K, Mohanty S K, Gupta P K, Arabale G V, Vijaymohanan K and Rao C N R 2006 *Opt. Express* **14** 424
- [23] Satishkumar B C, Thomas P J, Govindaraj A and Rao C N R 2000 *Appl. Phys. Lett.* **77** 2530